

Process design and optimization of pulsed electric fields treatment of microalgae

Justus Knappert¹⁾, Christopher McHardy¹⁾, Pauline Eppmann¹⁾, Tobias Horneber¹⁾, Alexander Jahn³⁾, Antonio Delgado^{2,3)} and *Cornelia Rauh^{1,3)}

¹⁾*Technische Universität Berlin, Department of Food Biotechnology and Food Process Engineering, Berlin, Germany*

²⁾*Friedrich-Alexander University Erlangen-Nuremberg, Institute of Fluid Mechanics, Erlangen, Germany*

³⁾*German Engineering Research and Development Center LSTME Busan Branch, 46742 Busan, Korea*

* cornelia.rauh@tu-berlin.de

Abstract

Due to their high production rates of proteins, fatty acids, pigments and other high value cell metabolites, microalgae are a promising resource for the food and feed, cosmetic and pharmaceutical industry. Since the downstream processing contributes largely to the overall production cost of microalgae-based products, new technologies are required to make intracellular substances accessible in an economical way. Due to its low energy requirements, the PEF technology was recently applied for cell disruption of different microalgae species, making various intracellular metabolites, like pigments and lipids, accessible for extraction. Nevertheless, most papers available are on a laboratory scale, using batch treatment chambers or continuous treatment chambers with a low mass flow rate.

This contribution demonstrates the possibilities of CFD-simulation as a tool for the optimization of PEF treatment chambers regarding a better treatment homogeneity. The investigated treatment chambers were designed on an industrial scale with a mass flow rate of 5000 kg h^{-1} . An ordinary colinear treatment chamber was compared to a modified treatment chamber. The modified arrangement has an additional displacer within the radial center of the high voltage electrode which was intended to improve the velocity distribution inside the treatment chamber. The simulation of both, the ordinary and the modified arrangement revealed a great benefit from the additional displacer. The velocity distribution across the radial coordinate was more homogeneous and dead zones and areas of recirculation within the high voltage electrode and after the isolators were avoided. As a result, the temperature increase, due to joule heating, was more moderate in the modified treatment chamber compared to the ordinary one. Therefore, the treatment of microalgae is better to control since the variance of the treatment conditions is smaller. With the presented modification, the risk of under- or over-processing and therefore, the loss of the process efficiency is reduced. Since the mass transfer enhancement for a following extraction step of temperature sensitive components is a major application of the PEF treatment of microalgae, the presented contribution provides a powerful tool for the process design and the upscale. Because

the impacts of single parameters are easy to investigate, a CFD-simulation of the process can help to save time and labor. Therefore, CFD-Simulation of the PEF process can contribute to help microalgae become a future resource for the food and feed, cosmetic and pharmaceutical industry.

Introduction

Due to their high production rates of proteins, fatty acids, pigments and other high value cell metabolites, microalgae are a promising resource for the food and feed, cosmetic and pharmaceutical industry. Nevertheless, until today the market breakthrough was not reached, mainly because of high production costs making microalgae not competitive compared to other sources for the prementioned nutrients. Since the downstream processing contributes largely to the overall production cost of microalgae-based products, new technologies are required to make intracellular substances accessible in an economical way. Due to its low energy requirements, the PEF technology was recently applied for cell disruption of different microalgae species, making various intracellular metabolites, like pigments and lipids, accessible for extraction. Most studies available are aiming towards pigments since those molecules can achieve a high marked price. (Luengo et al. (2014), Luengo et al. (2015)). It was shown that the extraction yield was enhanced, and that the PEF treatment did not cause any pigment degradation. This makes PEF inferior compared to other cell disruption technologies for the mass transfer enhancement during the extraction of pigments. Besides the pigments the substance group of the lipids is being met with considerable interest. Similar to pigments an significant increase of the extraction was demonstrated (Zbinden et al. (2013) Silve et al. (2018)) It was further shown by Zbinden et al. (2013) that the PEF treatment enabled the use of green solvents such as ethyl acetate. Since the PEF treatment enables the extraction from the wet biomass the mandatory and expensive drying step becomes obsolete (Silve et al. 2018). It was shown by different authors that the extraction of proteins is not improved by PEF in a way that a commercial application becomes reasonable (Lam et al. 2017, Pataro et al. 2017, Grimi et al. 2014). Nevertheless, PEF treatment can be applied for a selective extraction of proteins with a small molecule size. Martínez et al. (2017) showed promising results for the extraction of C- phycocyanin from *Arthrospira platensis*. An extraction yield of 70 % of the total cell content of C- phycocyanin was achieved after the PEF treatment. It was further shown that the purity of the gained extract was higher, and the cell size was much less affected through the PEF-treatment, compared to the cell disruption with bead milling. Therefore, a following separation step is facilitated through the PEF treatment.

All the scientific papers presented here show the great potential of the PEF technology for the downstream processing of microalgae. It could lower the mass transfer resistance for some molecules what makes other processing steps like drying or purification of the product unnecessary. But most of the presented studies have in common that the experiments were conducted on a laboratory scale in batch treatment chambers or continuous treatment chambers with a small mass flow. Since the electric field distribution is strongly depended on the electrode configuration and the treatment time is hard to control in a continuous treatment chamber, it is difficult to transfer those results on a larger scale. Since for industrial applications only continuous treatment

chambers are reasonable the scale up on such systems from laboratory experiments should be focused more. The most common type of continuous treatment chambers is the so called colinear arrangement. Its advantage is a high load resistance and therefore, a smaller current density is needed to apply the voltage which is needed to build up the wanted electric field strength (Jaeger et al. 2009). Its disadvantage on the other hand is the inhomogeneous distribution of the electric field which is stronger on the wall of the insulators and gets weaker to the center of the flow field. Since the flow velocity is higher in the center of the tube this effect is further enhanced. This could lead to an inadequate treatment in the middle of the tube and to an over processing at the wall. Since many targeting molecules from microalgae are temperature sensitive this should be avoided. This bottleneck for an industrial application can be solved by numerical simulation. Compared to experimental results, the numerical simulation provides local information about the electric field strength, the temperature and the velocity and can therefore be used as a tool to evaluate the effect of different treatment chamber designs. Several approaches to improve the treatment chamber design for a better treatment homogeneity can be found within the literature. Most of them are focusing on the influence of the isolator shape (Lindgren et al. 2002, Gerlach et al. 2008, Meneses et al. 2011). Jaeger et al. (2009), on the contrary did not vary the dimensions of the treatment chamber but added two grids made of either stainless steel or polypropylene respectively. The numerical simulation, including a suited turbulent model, revealed a better distribution of the velocity field, leading to a better treatment homogeneity. Nevertheless, it is questionable if such a grid is suitable for a long-term use for treating microalgae. Since precipitation at the electrodes is a serious problem while treating microalgae (Straessner et al. 2016) the grids can be clogged leading to a stop for the whole treatment process. Since the PEF-treatment of microalgae is independent of the biomass concentration for up to $160 \text{ g kg}_{\text{sus}}^{-1}$ (Goettel et al. 2013) this problem becomes even more relevant. Therefore, a grid electrode is not suitable for the treatment of microalgae suspensions. In contrast, the approach presented here surpasses this problem by adding an additional displacer at the middle line. This configuration allows a higher mass flow rate, even at higher biomass concentrations. The effect of the displacer on the electric field, temperature field and velocity field distribution was investigated in the presented study.

Material and Methods

Treatment Chamber Geometry and Experimental Setup

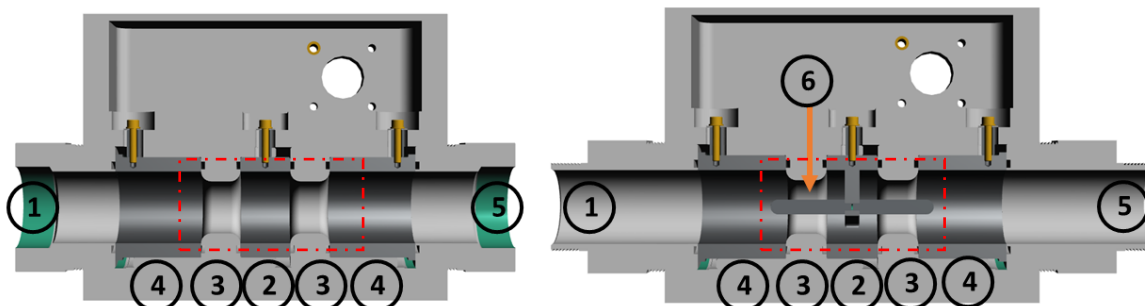


Figure 1: Investigated treatment chambers in this study. Left: ordinary colinear treatment chamber composed of two grounding electrodes (4), one high voltage electrode (2) and two isolator rings (3). Right: modified colinear treatment chamber with a cigar shaped displacer in the middle of the high voltage electrode and the isolator rings (6). The other parts of the treatment chamber are similar as in the ordinary one. The inlet of both chambers is on the left (1) and the outlet is on the right side (5). The inner diameter d_{IE} for ground and high voltage electrode for both chambers is 5 cm and the inner diameter for the isolator rings d_{II} is 3 cm. The flow direction for both chambers is from left to right. The red square symbolizes the section where contour plots are created to visualize the results of the simulation.

Within this study, the effect of different treatment chamber configurations on the electric field, temperature field and flow field were investigated by computational fluid dynamics simulations (CFD) using the open source software OpenFOAM. The different treatment chambers are presented in Figure 1. Crucial components are indicated by numbers. For both configuration the high voltage electrode (HVE) (2) is separated from the two grounding electrodes (1) by two isolator rings (3). Compared to the ordinary colinear treatment chamber presented on the left of Figure 1 the modified colinear treatment chamber has an additional displacer (4) in the middle of the HVE and the isolator rings. The inlet diameter for both configurations is 5 cm and a mass flow rate of $\dot{m} = 1.39 \text{ kg s}^{-1}$ was set. Since turbulence can occur at such high flow rates the Reynolds number was calculated at the inlet and inside of the isolators for both configurations. The resulting values were 35367 (inlet), 49121 (isolator, ordinary configuration) and 38443 (isolator, modified configuration) respectively. Therefore the k - ϵ -model with Reynolds-averaging-Navier stokes equations (RANS-equations) was chosen to describe the turbulent flow field. The influence of the electric field strength was tested by applying an electric potential at the electrode of 15 kV. A fixed pulse duration of $\tau = 100 \mu\text{s}$ and a frequency of $f = 80 \text{ Hz}$ were set. The inlet temperature was 283.15 K.

Governing Equations

The flow field, temperature field and the electric field occurring in a continuous PEF treatment chamber can be modeled by the conservation equations for mass, momentum, energy and charge. General assumptions which are made here are the incompressibility of the fluid, no time dependence change (steady state) and Newtonian behavior of the fluid. Since turbulence plays an important role in this simulation the velocity term U_i is decomposed into $U_i = \bar{U}_i + u_i$. Here the first term \bar{U}_i describes the mean value and u_i is a value for the velocity fluctuation around \bar{U}_i . Considering a constant density ρ the equation for mass conservation can be expressed as:

$$\rho \frac{\partial \bar{U}_j}{\partial x_j} = 0 \quad (1)$$

Here, x_j is the spatial coordinate in all three directions ($j = 1, 2, 3$). For the turbulent case, the Navier-Stokes equation for the momentum transport needs to be extended by the Reynolds Stress tensor $\rho \bar{u}_i \bar{u}_j$. Therefore, the equation for momentum conservation can be written as:

$$\rho \frac{\partial \bar{U}_i \bar{U}_j}{\partial x_j} = - \frac{\partial p}{\partial x_i} + \frac{\partial}{\partial x_j} \left(\mu \left(\frac{\partial \bar{U}_i}{\partial x_j} + \frac{\partial \bar{U}_j}{\partial x_i} \right) - \rho \bar{u}_i \bar{u}_j \right) \quad (2)$$

Here, buoyancy and any other source terms for the momentum were neglected and μ describes the viscosity of the fluid. The turbulence was included with the standard k - ϵ -model. Since ϵ describes the dissipation of the turbulent kinetic energy k into thermal energy also the balance equation for the internal energy is affected:

$$\rho c_p \frac{\partial T}{\partial t} + \frac{\partial}{\partial x_j} \left(-(\kappa + \kappa_T) \frac{\partial T}{\partial x_j} \right) + \rho c_p \frac{\partial \bar{U}_i T}{\partial x_j} = \pi_e \quad (3)$$

The dissipation is linked to Eq. (3) through the term κ_T which describes the turbulent heat conductivity and can be expressed as:

$$\kappa_t = c_p \mu_t = c_p \cdot \frac{C_\mu \rho k^2}{\epsilon} \quad (4)$$

Here, μ_t is the eddy viscosity and C_μ is a constant set to 0,09. Further terms in Eq. (3) are the heat capacity c_p , the thermal conductivity κ and the energy production term π_e . This term couples the electric field of the PEF treatment to the temperature field:

$$\pi_e = \sigma E^2 \cdot \tau f \quad (5)$$

Here, σ is the electric conductivity, E is the electric field strength, τ is the pulse width and f is the frequency. Finally, an equation describing the electric field needs to be found. This model equation is based on conservation of the free charge:

$$\frac{\partial J_i^{free}}{\partial x_i} = 0 \quad (6)$$

Following Ohm's law, the current density can be expressed with the electric field E and the electric conductivity σ as the constant of proportionality. Therefore, Eq. (6) becomes to:

$$\frac{\partial \sigma E_i}{\partial x_i} = 0 \quad (7)$$

Electrostatic fields are not only temporal constant but further free of rotation. Such a field can be described by the change of the electric potential Φ :

$$\frac{\partial \sigma E_i}{\partial x_i} = \frac{\partial}{\partial x_i} \sigma \frac{\partial \Phi}{\partial x_i} = 0 \quad (8)$$

If the electric conductivity is a constant, Eq. (8) becomes to the Laplace equation:

$$\frac{\partial}{\partial x_i} \frac{\partial \Phi}{\partial x_i} = \Delta \Phi = 0 \quad (9)$$

Since the boundary conditions for the electric potential at the electrode and the grounding are known, Eq. (9) can be solved.

Boundary Conditions

The boundary conditions for the whole model are presented in Table 1. The turbulence kinetic energy k for isotropic turbulence was estimated as a function of the given inlet velocity u_{ref} and an assumed degree of turbulence I of 5 %:

$$k = \frac{3}{2} (I |u_{ref}|)^2 \quad (10)$$

The turbulence dissipation rate ϵ was calculated as:

$$\epsilon = \frac{C_\mu^{0.75} k^{1.5}}{L} \quad (11)$$

Here, L is a reference length scale which is 5 % of the inlet diameter. At the inlet, the turbulent viscosity term μ_t and the thermal conductivity through the turbulent boundary layer α_t were set to zero. At the outlet, a fixed value for the pressure was given. All the other boundaries at the inlet and outlet respectively were described by a Neumann zero gradient boundary condition. The high voltage electrode (HVE), the groundings and the isolators were considered as walls for all flow related quantities and as adiabatic for the temperature flow. At the HVE and the grounding a fixed value for the electric potential of 15 kV and 0 kV was given respectively. In wall near regions all quantities related to the turbulence model were described by wall functions which are described in detail within the OpenFOAM user guide (OpenCFD Ltd).

Table 1: Boundary conditions as set within the CFD simulation using OpenFOAM. The near wall region was described by the standard wall functions of OpenFOAM. Their definition can be consulted in the OpenFOAM user guide (OpenCFD Ltd).

Property	P	T	U	Φ_E	ϵ	k	μ_t	α_t
Inlet	$\nabla P = 0$	283 [K]	0.7 [$\frac{m}{s}$]	$\nabla \Phi_E = 0$	0.0051 [$\frac{m^2}{s^3}$]	0.001838 [$\frac{m^2}{s^2}$]	0	0
Outlet	$P = P_{ref}$ [bar]	$\nabla T = 0$	$\nabla U = 0$	$\nabla \Phi_E = 0$	$\nabla \epsilon = 0$	$\nabla k = 0$	$\nabla \mu_t = 0$	$\nabla \alpha_t = 0$
HVE	$\nabla P = 0$	$\nabla T = 0$	0	15 [kV]	ϵ -Wall Function	$k_q R$ -Wall Function	$\mu_t k$ -Wall Function	α_t -Wall Function
Ground	$\nabla P = 0$	$\nabla T = 0$	0	0	ϵ -Wall Function	$k_q R$ -Wall Function	$\mu_t k$ -Wall Function	α_t -Wall Function
Isolator	$\nabla P = 0$	$\nabla T = 0$	0	$\nabla \Phi_E = 0$	ϵ -Wall Function	$k_q R$ -Wall Function	$\mu_t k$ -Wall Function	α_t -Wall Function

Material Properties and Process Parameters

Besides the boundary conditions, material properties are necessary to solve the governing equations. The governing Eq. (1), (2), (3), and (9) contain the properties: density (ρ), dynamic viscosity (μ), heat capacity (c_p), heat conductivity (κ) and the electric conductivity (σ). Within this study, fixed values where chosen which are summarized in Table 2.

Table 2: Material properties and PEF-Parameters expect the applied voltage and the inlet velocity used for the CFD simulation.

Property	Heat capacity	Dynamic viscosity	Heat conductivity	Density	Electric conductivity
Symbol	c_p	μ	κ	ρ	σ
Unit	$\left[\frac{\text{J}}{\text{kg K}} \right]$	$\left[\frac{\text{kg}}{\text{m s}} \right]$	$\left[\frac{\text{J}}{\text{s m K}} \right]$	$\left[\frac{\text{kg}}{\text{m}^3} \right]$	$\left[\frac{\text{S}}{\text{m}} \right]$
Value	4183	0.001	0.63	997	0.28

Computational Methods

The mesh was generated with the snappyHexMesh tool of the open source software OpenFOAM v5. This software, based on finite volume methods, was later used to solve the above equations with a modified version of the buoyantSimpleFoam. The modification of the solver was the addition of the equation for the electric field and the additional source term in the energy equation.

Indicator Functions

To compare the different geometries regarding their treatment homogeneity the mean value and the standard deviation of the electric field, temperature field and velocity field and the resulting coefficients of variation were used as indicators. The standard deviation X_{SD} for those quantities as described by Gerlach et al. (2008) has the form:

$$X_{SD} = \sqrt{\frac{1}{V_{gap}} \sum_1^N (X_i - X_{mean})^2 \delta V_i} \quad (12)$$

Here, V_{gap} is the Volume of the insulator gap where the electric field is active. N is the number of finite volume elements within this gab, X_i is the strength of the considered quantity in each of those elements and V_i is the volume of one element. X_{mean} is the average of the considered quantity within the insulator gap. It can be calculated as:

$$X_{mean} = \frac{1}{V_{gap}} \sum_1^N X_i \delta V_i \quad (13)$$

The volume of the treatment chamber is the sum of all finite volume elements:

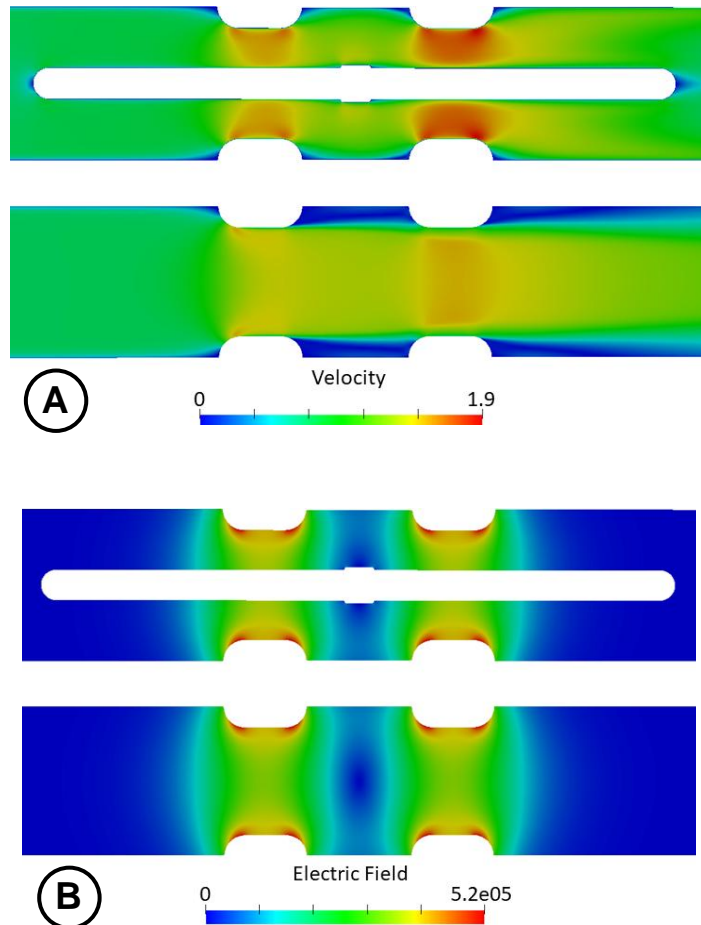
$$V_{gap} = \sum_1^N \delta V_i \quad (14)$$

Finally, a coefficient of variation can be defined to compare different set ups:

$$X_{CV} = \frac{X_{SD}}{X_{mean}} \quad (15)$$

In this study X was either the electric field strength E , the temperature T , or the velocity U .

Results and Discussion



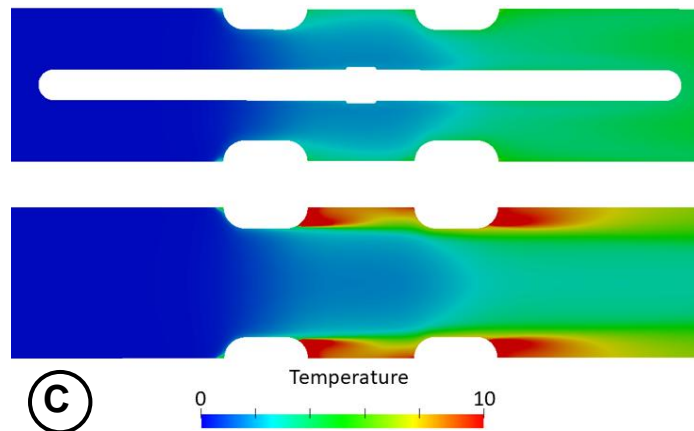


Figure 2: Contour plots of the velocity field (A), electric field (B) and temperature field (C). The contour plots are showing the section of the treatment chamber which is marked by a red square in Figure 1. The upper row represents the modified treatment chamber configuration with displacer whereas the lower one represents the ordinary colinear treatment chamber. The flow is from the left side to the right.

The results from the case study are presented as contour plots in Figure 2. The plots show the section which is indicated as a red square in Figure 1. It can be seen from plot A that the velocity is higher within the isolator gap of the modified treatment chamber compared to the ordinary one. This is not surprising since conservation of mass needs to be valid. Nevertheless, the velocity distribution is more homogeneous for the modified treatment chamber. In the ordinary treatment chamber large boundary layers occur, which is indicated by the green layers in plot A of Figure 2. In the modified treatment chamber, this boundary layers are much thinner, which leads to a smaller gradient of the velocity along the radial coordinate and therefore, to a more homogeneous velocity distribution. This is also expressed in the indicators for the velocity, listed in Table 3. The mean velocity for the ordinary treatment chamber inside the isolator gaps was 1.25 m s^{-1} and 1.24 m s^{-1} for the first and the second isolator respectively. For the modified treatment chamber, the mean velocity was 1.33 m s^{-1} and 1.34 m s^{-1} for the first and the second isolator. Nevertheless, the standard deviation for the velocity was 0.28 and 0.34 for the ordinary treatment chamber and 0.26 and 0.30 for the modified treatment chamber respectively. Therefore, the coefficients of variation were lower for the modified treatment chamber inside both isolators (see Table 3). Another advantage of the displacer regarding the flow field can be seen in Figure 3. As indicated by the streamlines, large areas of recirculation occur inside the high voltage electrode for the ordinary treatment chamber design. Furthermore, after the second isolator, large dead zones appear. Both, the zones of recirculation and dead flow areas are leading to long residence times which can cause an over processing of the product. As shown in Figure 3 those zones are not appearing inside the modified treatment chamber. Since the heating of the fluid through the electric energy input is a function of the residence time, the zones of recirculation have a large influence on the temperature increase. As it

can be seen from Figure 2 (C), the temperature increase was the highest at the spots were the recirculation areas occur. Inside the high voltage electrode and after the second isolator the temperature increase was 10 K or higher for the ordinary treatment chamber. Inside the modified treatment chamber, the temperature increase was around 5 K. Since the mass transfer enhancement for subsequent extraction steps of temperature sensitive products is an important application of the PEF-treatment of microalgae, this is a very important result of the presented work. The effect of the displacer on the temperature also expressed in the mean temperature T_{mean} , the standard deviation T_{SD} and the coefficient of variation T_{CV} (see also Table 3). Since those values are calculated for the isolator gaps and as mentioned before the temperature increase is most important inside the high voltage electrode and after the second isolator, the effect of the displacer on those values is not very high. Nevertheless, maximum temperature was 313.27 K and 305.5 K for the ordinary treatment chamber inside the first and the second isolator respectively and 293.86 K and 298.13 K for the modified treatment chamber. This can be explained by the higher velocities and the thinner boundary layer inside the isolators of the treatment chamber with the displacer. Because of this, the heat transfer from the fluid at the wall is higher towards the turbulent flow in the middle of the isolator. Moreover, the standard deviation for the temperature was 1.05 K and 1.27 K for the first and the second isolator in the modified treatment chamber respectively. On the contrary the standard deviation was 3.35 K and 2.60 K inside the isolators of the ordinary treatment chamber. Overall, this means a more homogeneous treatment of the product, in our case the microalgae suspension. The temperature stress is decreased, which is a great advantage if a temperature sensitive product shall be extracted afterwards.

Since the electric field strength in a colinear treatment chamber is stronger at the wall of the isolators and weaker towards the middle of the isolator, the presented displacer improves the homogeneity of the electric field in an indirect way. Because the displacer is made of isolating material itself, it has no direct influence on the electric field. Nevertheless, the area with the weakest field strength is simply cut off by the displacer and therefore, the homogeneity is improved. This is also expressed in the indicator numbers as it leads to a slight improvement of the mean field strength from $3.6e05 \text{ Vm}^{-1}$ in the ordinary treatment chamber to $3.7e05 \text{ Vm}^{-1}$ in the modified treatment chamber. Also, the standard deviation was a bit lower and therefore, the coefficient of variation decreased from 0.135 to 0.128 for the ordinary treatment chamber and the modified treatment chamber respectively. Note that the temperature dependency of the electric conductivity was not considered in this case study due to the large computational resources needed for the turbulent flow field. Therefore, the electric field strength was almost the same in both isolator gaps for each treatment chamber. If the temperature dependency is considered, the electric conductivity would increase in positive x-direction due to the previously described temperature increase. This would lead to a decreased field strength within the second isolator gap. As discussed before, the temperature increase is more moderate in the second isolator gap of the modified treatment chamber, compared to the ordinary one. Therefore, the difference between the mean field strength would be smaller between the two isolator gaps in the modified treatment chamber compared to the ordinary one.

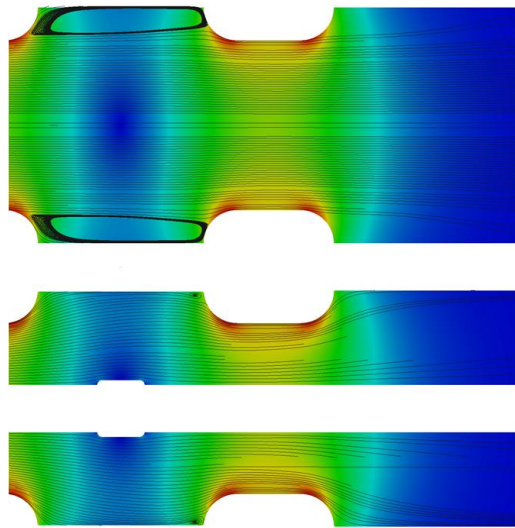


Figure 3: Contour plot and streamlines for the ordinary colinear treatment chamber (upper) and the modified treatment chamber (lower). The section shows the high voltage electrode, the second isolator gap and the second grounding electrode. Large areas of recirculation are revealed by the streamlines for the ordinary colinear treatment chamber inside the high voltage electrode.

Table 3: Comparative values for the electric field strength E , the temperature T and the velocity U calculated by Eq.s (12), (13) and (15) inside the first and the second isolator (ISO 1 and ISO 2) for the ordinary and modified colinear treatment chamber respectively.

	Ordinary ISO 1	Ordinary ISO 2	Modified ISO 1	Modified ISO 2
E_{max} $\left[\frac{V}{m}\right]$	5.18e05	5.18e05	5.46e05	5.22e05
E_{mean} $\left[\frac{V}{m}\right]$	3.60e05	3.60e05	3.66e05	3.67e05
E_{SD} $\left[\frac{V}{m}\right]$	0.49e05	0.49e05	0.47e05	0.47e05
E_{CV} [-]	0.135	0.136	0.128	0.128
T_{max} [K]	313.27	305.55	293.86	298.13
T_{mean} [K]	284.84	287.18	284.38	284.88
T_{SD} [K]	3.35	2.60	1.05	1.27
T_{CV} [-]	0.01	0.01	0.004	0.004
U_{max} $\left[\frac{m}{s}\right]$	1.49	1.49	1.66	1.88

U_{mean} $\left[\frac{m}{s}\right]$	1.25	1.24	1.33	1.34
U_{SD} $\left[\frac{m}{s}\right]$	0.28	0.34	0.26	0.30
U_{CV} [-]	0.22	0.27	0.20	0.22

The presented work shows the great potential of CFD simulation for the improvement of the treatment chamber design for a more homogeneous treatment. The modified treatment chamber has a better treatment homogeneity, mainly due to the improvement of the flow field. As a result, the temperature increases inside the high voltage electrode and after the second isolator are minimized. Furthermore, the electric field is more homogeneous because the area with the lowest field strengths is cut off by the displacer. Nevertheless, for the treatment of microalgae, the mean electric field strength of $3.66e05 \text{ V m}^{-1}$ is too low. Luengo et al. (2014) reported that at least $1e06 \text{ V m}^{-1}$ in a parallel plate batch treatment chamber are necessary for the irreversible perforation of *Chlorella vulgaris* cells. Since a long treatment time of $150 \mu\text{s}$ is needed for this field strength an even higher field strength of $1.5 - 2.0e06 \text{ V m}^{-1}$ should be applied in a continuous colinear treatment chamber. Besides simply applying higher voltages, which is limited by the pulse generator on an industrial scale, this can be done by varying the isolator length and diameter (Gerlach et al. 2008). Therefore, the presented modified treatment chamber should be further optimized with this approach. Since closed cultivation systems for microalgae can have a volume of more than 1300 m^3 (a4f), the presented mass flow rate of 5000 kg h^{-1} is needed for a fast processing. Even if the algae suspension is concentrated by a factor of 100, 2.6 h are needed to process the whole biomass. For open pond systems, which have a much larger volume, it is even more crucial to have a treatment chamber with a high mass flow rate, as the presented one. This demonstrates the industrial relevance of the presented work, since CFD-simulation of PEF provides a powerful tool for the upscaling of treatment chambers.

Publication bibliography

a4f, Large Industrial Projects. ALGAFARM SECIL / ALLMICROALGAE. Available online at <https://www.a4f.pt/en/projetos/algafarm>, checked on 7/11/2019.

Gerlach, D.; Alleborn, N.; Baars, A.; Delgado, A.; Moritz, J.; Knorr, D. (2008), Numerical simulations of pulsed electric fields for food preservation: A review, *Innovative Food Science & Emerging Technologies*, Vol.9(4), 408–417.

Goettel, M.; Eing, C.; Gusbeth, C.; Straessner, R.; Frey, W. (2013), Pulsed electric field assisted extraction of intracellular valuables from microalgae, *Algal Research*, Vol.2(4), 401–408.

Grimi, N.; Dubois, A.; Marchal, L.; Jubeau, S.; Lebovka, N. I.; Vorobiev, E. (2014), Selective extraction from microalgae *Nannochloropsis* sp. using different methods of cell disruption, *Bioresource technology*, Vol.153, 254–259.

Jaeger, H.; Meneses, N.; Knorr, D. (2009), Impact of PEF treatment inhomogeneity such as electric field distribution, flow characteristics and temperature effects on the inactivation of *E. coli* and milk alkaline phosphatase, *Innovative Food Science & Emerging Technologies*, Vol.**10**(4), 470–480.

Lam, G. P.t.; Postma, P. R.; Fernandes, D. A.; Timmermans, R.A.H.; Vermuë, M. H.; Barbosa, M. J. et al. (2017), Pulsed Electric Field for protein release of the microalgae *Chlorella vulgaris* and *Neochloris oleoabundans*, *Algal Research*, Vol.**24**, 181–187.

Lindgren, M.; Aronsson, K.; Galt, S.; Ohlsson, T. (2002), Simulation of the temperature increase in pulsed electric field (PEF) continuous flow treatment chambers, *Innovative Food Science & Emerging Technologies*, Vol.**3**(3), 233–245.

Luengo, E.; Condón-Abanto, S.; Álvarez, I.; Raso, J. (2014), Effect of pulsed electric field treatments on permeabilization and extraction of pigments from *Chlorella vulgaris*, *The Journal of membrane biology*, Vol.**247**(12), 1269–1277.

Luengo, E.; Martínez, J. M.; Bordetas, A.; Álvarez, I.; Raso, J. (2015), Influence of the treatment medium temperature on lutein extraction assisted by pulsed electric fields from *Chlorella vulgaris*, *Innovative Food Science & Emerging Technologies*, Vol.**29**, 15–22.

Martínez, J. M.; Luengo, E.; Saldaña, G.; Álvarez, I.; Raso, J. (2017), C-phycocyanin extraction assisted by pulsed electric field from *Artrosphaera platensis*, *Food research international (Ottawa, Ont.)*, Vol.**99**(Pt 3), 1042–1047.

Meneses, N.; Jaeger, H.; Moritz, J.; Knorr, D. (2011), Impact of insulator shape, flow rate and electrical parameters on inactivation of *E. coli* using a continuous co-linear PEF system, *Innovative Food Science & Emerging Technologies*, Vol.**12**(1), 6–12.

OpenCFD Ltd, User Guide. Available online at
<https://www.openfoam.com/documentation/user-guide/index.php>, checked on 6/20/2019.

Pataro, G.; Goettel, M.; Sträßner, R.; Gusbeth, C.; Ferrari, G.; Frey, W. (2017), Effect of PEF Treatment on Extraction of Valuable Compounds from Microalgae *C. vulgaris*, *Chemical Engineering Transactions*, Vol.**57**, 67–72.

Silve, A.; Papachristou, I.; Wüstner, R.; Sträßner, R.; Schirmer, M.; Leber, K. et al. (2018), Extraction of lipids from wet microalga *Auxenochlorella protothecoides* using pulsed electric field treatment and ethanol-hexane blends, *Algal Research*, Vol.**29**, 212–222.

Straessner, R.; Silve, A.; Eing, C.; Rocke, S.; Wuestner, R.; Leber, K. et al. (2016), Microalgae precipitation in treatment chambers during pulsed electric field (PEF) processing, *Innovative Food Science & Emerging Technologies*, Vol.**37**, 391–399.

Zbinden, M. D. A.; Sturm, B. S. M.; Nord, R. D.; Carey, W. J.; Moore, D.; Shinogle, H.; Stagg-Williams, S. M. (2013), Pulsed electric field (PEF) as an intensification

*The 2019 World Congress on
Advances in Nano, Bio, Robotics and Energy (ANBRE19)
Jeju Island, Korea, September 17 - 21, 2019*

pretreatment for greener solvent lipid extraction from microalgae, *Biotechnology and bioengineering*, Vol.**110**(6), 1605–1615.